Surface Energy, Its Density and Distance: New Measures with Application to Human Cerebral Potentials

Wenyu Wang, Henri Begleiter, and Bernice Porjesz

Summary: In this paper, we propose three new measures for topographic studies of event related potentials (ERP) called the surface energy (SE), its density (SED) and the distance of surface energy density fields (DSED) based on the entire scalp current density (SCD) field. These measures have a specific physical meaning, are free of the reference electrode and any physical conductive model of the head. They capture not only spatial properties, but also continuous time elements present and smeared in the original scalp potential records. They provide a common base for comparisons of recorded potentials among different time points, subjects, regions on the scalp, or experimental conditions. We also construct a statistical inference based on these new measures, and provide an application to human event-related potentials in a visual short-term memory experiment.

Key words: Surface energy; Surface energy density; Distance of surface energy density fields; Visual short-term memory.

Introduction

Choosing spatial or time measures for recorded neurophysiological data is a fundamental problem in topographic studies of EEG and ERP. Almost all efforts in topographic analyses have been directed at the potentials themselves or some extracted functions of the potentials, such as component amplitudes and latencies, autocorrelation, crosscorrelation (Gevins 1987), the global field power (GFP) and the global dissimilarity (GD) (Lehmann and Skrandies 1980; Lehmann 1987). Unfortunately, most measures provided in the literature are not reference free measures. Actually, the recorded potentials are the potential differences between recorded electrodes and the reference electrode, and the location of the reference electrode is usually not far enough from all potential source to be considered a "quiet reference" (Nunez 1981). Most measures provided in the literature depend on placement of the reference electrode in different experiments, which may change for different subjects and at different time points as the potential of the reference electrode varies. For instance, the components themselves, the autocorrelations and crosscorrelations will change if the placement of the reference electrode is changed or the reference electrode is not a "quiet reference." Therefore, these measures cannot be used for comparisons of the recorded potentials among different subjects, time points or experimental conditions since they are not derived from a common base. This problem is even more severe in the case in which more than one electrode is used. The analysis based on these measures may lead to false conclusions. In addition to this reference electrode problem, the global field measures provided in the literature such as the global dissimilarity and the GFP lose physical meaning for the scalp potential (SP) field, treat the potentials recorded at different electrode sites as spatially undifferentiated and use only these finite records.

Let $A_1, A_2,...,A_n$ and $B_1, B_2,...,B_n$ be recorded potentials at n electrode sites on the scalp for map A and map B, respectively. Then for the global dissimilarity of these two maps $GD(A,B)$, we have $GD(A,B)^2 = 2^* (1\text{-}r(A,B))$ where $r(A,B)$ is the sample correlation of the two sets of recorded potentials. Therefore $GD(A,B)$ represents the linear relationship of map A and map B. The GFP(A) is the standard deviation of the recorded potentials at n electrode sites for map A vs. their average, and $\sqrt{n}$GFP(A) is independent of n if we assume the recorded potentials at n electrode sites have the same mean. Such finite, local and spatially equally treated records may not capture all the important properties in the entire scalp potential (SP) field as illustrated in figure 1, which shows the SP fields

Neurodynamics Lab, Department of Psychiatry, SUNY Health Science Center at Brooklyn, New York.

Accepted for publication: June 10, 1993.

This work was supported by N.I.H. grants AA-02686 and AA-05524.

Correspondence and reprint requests should be addressed to Wenyu Wang, Ph.D., Neurodynamics Lab., Box 1203, Department of Psychiatry, SUNY Health Science Center at Brooklyn, 450 Clarkson Ave., Brooklyn, NY 11203, U.S.A.

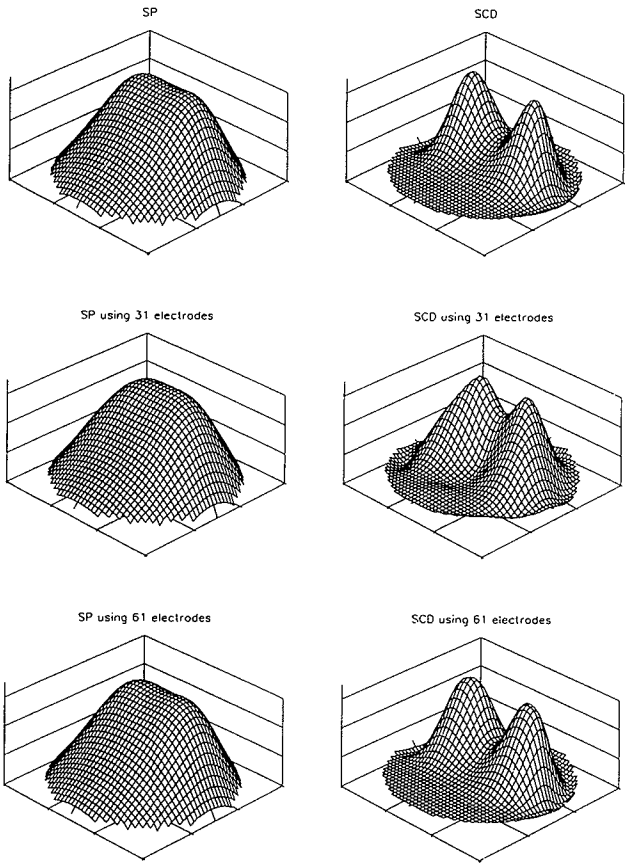

Figure 1. SP fields and their corresponding SCD fields. The fields at the top are created by using the one-shell model and two symmetric dipoles with nominal position

$$(r_p, f_p, t_p) = (0.519, 0.2\pi, +- \frac{1}{3}\pi)$$

and nominal moment $(r_m, f_m, t_m) = (0.5, 0, 0)$. The fields at the middle and the bottom are obtained by using the same model and dipoles to obtain values of SP at 31 electrode sites and 61 electrode sites, respectively, then interpolating these values by the spherical spline method.

and their corresponding scalp current density (SCD) fields. It is clear that interpolated SP and SCD fields are closer to the true SP and SCD fields by using potentials at 61 electrode sites than by using potentials at 31 electrode sites. This also shows that using records at the finite electrode sites may not capture all the important properties of the SP or SCD field.

In practice, SP's are only recorded at finite electrode sites. Therefore, an SP field on the whole scalp can only be obtained through some interpolating techniques. The method we used in this paper is the spherical spline method (Wahba 1981; Perrin 1989). Due to the properties of the spline, the interpolated SP or SCD field (by using recorded potentials at the electrode sites on the scalp) is a good approximation of the true SP or SCD field if the number of sites is large enough. Therefore, it is reasonable to assume that a global measure based on the entire interpolated SP or SCD field should represent the true SP or SCD field better than that based on only finite electrode sites.

We propose three new measures called the surface energy (SE), its density (SED) and the distance of surface energy density fields (DSED) based on the spherical spline and the entire interpolated SCD (the surface Laplacian of scalp potential) field. The SE gives a global field measure and an SE wave in a time interval shows continuous time elements and can for example be used in topographic component recognition. The SED indicates the amount and scalp distribution of SE at a fixed time. An SED field also represents its corresponding SCD field in accordance with Definition **B**. The DSED measures the pattern difference of two surface energy density fields (or in some sense the two corresponding SCD fields), and can be used in topographic component and pattern recognition. The corresponding local SE, SED and DSED can also be used in local comparisons among different regions on the scalp. These measures have a specific physical meaning and have all the advantages of SCD, such as being free of any physical conductive models of the head and independent of the reference electrode. They provide a common base for comparison among different subjects, time points, regions on the scalp or experimental conditions. Moreover, they retain not only the spatial properties, but also the existent continuous time elements typically smeared in the original potential records. We also provide a statistical inference based on the proposed approach.

The surface energy and its density and distance

In this section, we use a rectangular coordinate system with origin O at the center of the sphere, the x-axis passing through the inion, the y-axis passing through the right ear, and the z-axis going through the vertex. We assume the portion of the head under 10-20 electrode placements is a hemisphere of radius 1.

It is well known that the SCD field generated from the interpolated SP field by potentials measured with electrodes on the scalp acts as a spatial filter, which emphasizes local sources over distant sources and provides significant improvement in spatial resolution (Nunez et al. 1991). It is independent of any physical conductive model of the head. The physical interpretation of SCD is that it provides an estimate of local skull current flow from the brain into the scalp (see e.g., Nunez 1981; Perrin 1987).

In practice, SP's are only recorded at finite electrode sites; however, various interpolating techniques can be used to get a SP field on the whole scalp. Here we use the spherical spline method (Wahba 1981; Perrin 1989) to get a SP field, obtained by finding a smoothing spline on the sphere with the smallest bending energy, and passing through the recorded potential at electrode sites on the scalp. Let v_i be the potential value recorded at the ith electrode on the scalp whose spherical projection is E_i. Then the spherical spline potential (SSP) $SSP(P)$ at a point P on the sphere is given by

$$SSP(P) = SSP(x,y,z) = c_o + \sum_{i=1}^{q} c_i\, g(\cos(\gamma(P,E_i))), \tag{2.1}$$

where q is the total number of electrodes on the scalp and the c_i's are solutions of

$$\left.\begin{aligned} GC + U c_o &= V, \\ U^T C &= O, \end{aligned}\right\} \tag{2.2}$$

with

$$\mathbf{U}^T = (1,1,\ldots,1),\ \mathbf{C}^T = (c_1, c_2,\ldots,c_q),$$

$$\mathbf{V}^T = (v_1, v_2,\ldots, vq),\ \mathbf{G} = (g_{ij}) = (g(\cos(\gamma(E_i, E_j)))),$$

$$g(\cdot) = \frac{1}{4\pi} \sum_{n=1}^{\infty} \frac{2n+1}{n^m (n+1)^m} P_n(\cdot), \tag{2.3}$$

where $P_n(.)$ is the nth Legendre polynomial and m is the smoothing parameter (usually equals 3).

The corresponding SCD field can be obtained from (2.1) (see Appendix for details) as follows, assuming m >2,

$$SSCD(P) = \sigma_1 \sum_{i=1}^{q} c_i\, h(\cos(\gamma(P, E_i))), \tag{2.4}$$

$$h(\cdot) = \frac{1}{4\pi} \sum_{n=1}^{\infty} \frac{2n+1}{n^{m-1}(n+1)^{m-1}} P_n(\cdot). \tag{2.5}$$

Now, we define the SE and SED as follows.

Definition A.

$$SE = \int_o^{2\pi} \int_o^{\frac{\pi}{2}} (SSCD(\varphi,\theta))^2 \sin(\varphi)\, d\varphi d\theta \tag{2.6}$$

Definition B.

$$SED(P) = SED(1,\varphi,\theta) = (SSCD(P))^2 \sin(\varphi)/SE, \tag{2.7}$$

$$\varphi \in [0, \frac{\pi}{2}],\ \theta \in [0, 2\pi]$$

Similarly, we can define the local SE and SED (LSE and LSED) on a region **U** in the latitude and longitude domain by changing the domain of the integral in (2.6) and the domain in (2.7) to the **U**. Let

$$F = \{P_{ij}(1, \varphi_i, \theta_j),\ \varphi_i \in [0, \frac{\pi}{2}],\ \theta_j \in [0, 2\pi],$$
$$i = 0, 1,\ldots, m;\ j = 0, 1,\ldots, n\}$$

be a grid with equal $\Delta\varphi$ in latitude φ and equal $\Delta\theta$ in longitude θ on the hemisphere. Then we can approximate

$$SE \approx \sum_{i=1}^{m} \sum_{j=1}^{n} (SSCD(\tilde{P}_{ij}))^2 \sin(\tilde{\varphi}_i)\, \Delta\varphi\Delta\theta, \tag{2.8}$$

where $\tilde{P}_{ij}$ with latitude $\tilde{\varphi}_i \in (\varphi_{i-1}, \varphi_i)$ and longitude $\tilde{\theta}_j \in (\theta_j - 1, \theta_j)$

If we denote

$$\tilde{\Delta} \overset{def}{=} \frac{1}{\sin^2\varphi} \frac{\partial^2}{\partial\theta^2} + \frac{1}{\sin\varphi} \frac{\partial}{\partial\varphi} \left(\sin\varphi \frac{\partial}{\partial\varphi}\right)$$

as the restriction of the Laplacian in 3-dimensional space to the surface of the sphere, then

$$SE = \int_0^{2\pi} \int_0^{\frac{\pi}{2}} (\tilde{\Delta} SSP)^2 \sin(\varphi)\, d\varphi d\theta$$

which may be considered to be the analogue of the bending energy of a thin plate (Wahba 1981) or the bending energy of the SP field. It is clear that SE is a global measure and a function of the recorded potentials at electrode sites on the scalp through the SSP field. Therefore, we can look to the surface energy as a kind of weighted summation of the recorded potentials, and the weights themselves represent the advantage of spline, the spatial information of the sites and the bending energy of the SP field. It should be indicated here that SE is not the energy of an electric field in a general sense (see e.g. Nunez 1981). SE is different from the measures provided in the literature in its combined advantages. SE is reference independent and free of any physical conductive model of the head. SE represents the bending energy of the SP field while the GFP is the standard deviation of recorded potentials at electrode sites vs. their average. SE uses the entire SP field and treats potentials at different positions differently, while the GFP uses only the recorded potentials at finite electrode sites and treats these records spatially equally. As we showed in figure

1, using spatially equally treated records at the finite electrode sites may not capture all the important properties of the SP or SCD field. From an SE wave in a time interval, we can define, for example, the surface energy components (SEC) based on peaks in the wave.

The SED measures the distribution of the SE on the scalp. An SED field also represents its corresponding SCD field in the sense of Definition **B**. The peaks of SED in a region on the scalp represent the peaks or valleys of the corresponding SCD in the region. SED has all the advantages of SCD, but is a scale-invariant measure while SCD is not. A set of successive SED maps obtained from recorded potentials in an experiment will give the corresponding brain activity for the experiment. The corresponding LSE and LSED give local measures of the SE and SED, and can be used for the problem involved in some regions on the scalp.

For topographic pattern and component recognition, we define the DSED as follows:

Definition C.

Let SED1 and SED2 be two surface energy densities. We define the DSED of these two densities as

$$DSED = \left(\int_0^{2\pi} \int_0^{\frac{\pi}{2}} ((SED1\ (\varphi,\theta))^{1/2} - (SED2\ (\varphi,\theta))^{1/2})^2\, d\varphi d\theta \right)^{1/2}. \tag{2.9}$$

Similarly, we can define the local DSED (LDSED) on the region **U** and an approximate formula for the DSED. Such distance between density functions of two random variables is called Hellinger distance in statistics which represents the total variation of the two distributions (see Devroye 1987 for details). The DSED is scale-invariant. Since an SED field represents its corresponding SCD field above-mentioned, the DSED of two SED fields represents the pattern difference of the two corresponding SCD fields. In contrast, the global dissimilarity *GD(A,B)* of map A and map B represents only the linear relationship between map A and map B. The DSED uses the entire SP field and treats potentials at different position differently, while the GD uses only the recorded potentials at the finite electrode sites and treats these records spatially equally. As we showed in figure 1, using spatially equally treated records at the finite electrode sites for a distance measure may not capture all the important differences of two SP or SCD fields. A wave of the DSED between successive surface energy fields in a time interval gives the field configuration. Peaks in this wave show large pattern changes between the successive surface energy density fields or the corresponding successive SCD or SP fields. The band of a surface energy component may be defined based on both the corresponding peak in the SE wave and the corresponding peaks and flat interval in the DSED wave. Clearly, the SE, SED and DSED can be used as measures in comparing different subjects, time points, experimental conditions, or regions on the scalp.

For easy reference, we summarize the calculation steps of the SE, SED and DSED as follows:
(1). Evaluate g function in (2.1) and h function in (2.5) at the spherical projections Ei's of electrode locations and also evaluate h function at all points of the grid F on the hemisphere (need to be performed only once).
(2). Use potentials recorded at electrode sites on the scalp and (2.2) to derive c's.
(3). Use (2.4) to calculate SCD at all points of the grid F on the hemisphere.
(4). Use (2.8) ((2.7)) to calculate the SE (the SED) at different time points or different experiments.
(5). Use (2.9) to calculate the DSED between two different time points or two different experiments.

Statistical inference based on the SE, SED and DSED.

Here, we show one example for statistical inference based on the SE. The same idea can be applied to the SED and the DSED. Let $SE_i\ (t)$, $i = 1, 2,..., m$; $t = 1, 2,...,n$ be the SE from the recorded potentials in different cases i's and time t's. Assume

$$SE_i\ (t) = f_i\ (t) + \zeta_i(t),\ i = 1, 2,..., m;\ t = 1, 2,..., n, \tag{2.10}$$

where $f_i(t)$ are determined functions of t, $\zeta_i\ (\cdot)$, $i = 1, 2,...,$ m, are independent and for each i, $\zeta_i\ (t)$, $t = 1, 2,..., n$, are *iid* random variables with mean zero and variance σ_i^2. To test, for example, $f_1(\cdot) = f_2(\cdot)$, we can construct the following statistic:

$$T = n^{1/2} \frac{MDSE}{SDSE}, \tag{2.11}$$

where

$$MDSE = \frac{1}{n} \sum_{t=1}^{n} (SE_1\ (t) - SE_2\ (t)),$$

$$SDSE = \left(\frac{1}{(n-1)} \sum_{t=1}^{n} (SE_1\ (t) - SE_2\ (t) - MDSE)^2 \right)^{\frac{1}{2}} \tag{2.12}$$

It is well known that if we assume ζ_1 and ζ_2 are Gaussian processes, then the statistic T has the t-distribution with n-1 degree of freedom.

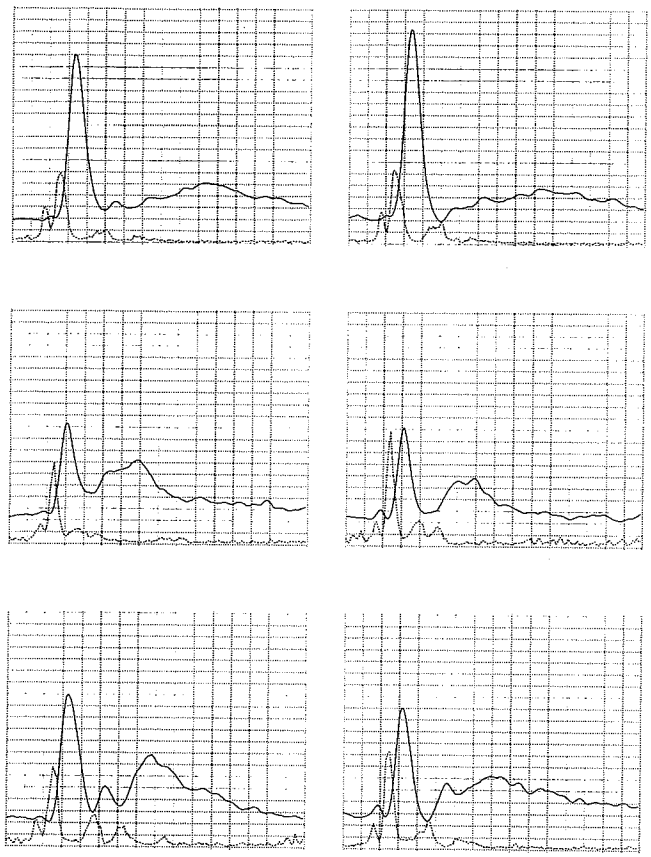

Figure 2. SE waves and DSED waves (the value of the DSED between successive surface energy fields is multiplied by 10^6 in order to compare it with the SE) in the six cases: the simple case is at the top left, the simple-matching case is at the middle left, and the simple-nonmatching case is at the bottom left; on the right side are the corresponding three complex cases. Solid lines are the SE waves; dashed lines are the corresponding DSED waves. The interval between two adjacent reference lines at the time-axis (horizontal axis) is 50 ms.

Application

In this section, we apply the new measures SE, SED and DSED to an analysis of human ERP obtained in a visual short-term memory experiment (Begleiter et al. 1993). In this experiment, 25 healthy volunteers (mean age = 20.3) participated. Each individual was fitted with the 32 lead scalp electrode cap (Standard Electrode Position Nomenclature, American EEG Society, Dec., 1990). All scalp electrodes were referred to Cz. Trials with excessive eye movements (> 75 μV) were eliminated from the final average. The electrical activity recorded at each electrode was fed to a set of amplifiers (Sensorium EPA-2) with a 10,000 gain and a bandpass of 0.02-50 Hz. The data were digitally filtered with a 30 Hz cutoff.

A modified delayed matching-to-sample task paradigm was used in which two visual stimuli were presented in succession with a 1.5 s fixed interstimulus interval. A trial consisted of a rectangular frame which was presented on the computer display 500 ms before the appearance of the first visual pattern (S1), and remained on the screen for another 900 ms after the presentation of the second visual pattern (S2). The visual frame was presented to indicate the beginning and end of a trial. The inter-trial interval was 4.5 s. The visual stimuli (100 ms duration) subtended a visual angle between 3 and 6 degrees. The stimuli consisted of simple visual line patterns (comprised of a few line elements) and complex patterns (comprised of a greater number of elements). These stimuli were selected to be difficult to name, that is lacking simple verbal descriptors. Consequently the mnemonic processes involved were not likely to be semantically mediated. A total of 70 simple and 70 complex visual patterns were randomly presented as training stimuli (S1). On half of the trials, the test stimuli (S2) were identical to S1; on the other half of the trials, the S2 stimuli were distinctly different from S1. The simple S1 stimuli were always followed by simple matching or nonmatching S2 stimuli, while the complex S1 stimuli were followed by complex matching or nonmatching S2 stimuli. The presentation of trials with simple and complex stimuli was randomized as were trials with matches and nonmatches.

On each trial, after the presentation of S2, the subject was asked to press a microswitch in one hand if S2 matched S1, and to press a microswitch in his other hand if S2 differed from S1 (choice reaction time). The designation of the hand indicating match or nonmatch was alternated across subjects. Accuracy and speed were equally emphasized.

The ERP's were recorded for 6 cases: simple training, complex training, simple-matching, simple-nonmatching, complex-matching and complex-nonmatching. For each case, 280 points sampled every 5.2 ms were used for the SE and SED calculation. Each sample contained 31 grand averages of ERP's (averaging over trials and 25 subjects) recorded at 31 electrode sites. A grid

$$F = \{P_{ij}(1,\varphi_i,\theta_j),\ \varphi_i = \frac{i\pi}{40},\ i = 1, 2,..., 20;\ \theta_j = \frac{j\pi}{40},\ j = 0, 1,..., 79\}$$

consisting of 1600 equally divided points was chosen for approximating the SE and SED.

The SE, SED and DSED are reference-free measures, so that their figures are comparable among different time points and different cases. From figure 2, two SECs, SEC175 (125-225 ms) and SEC375 (250-500 ms), can be identified, since they are related to the peaks in the SE wave and the peaks and flat intervals in the DSED wave. It can very clearly be seen in the 6 cases that: (1) SEC175

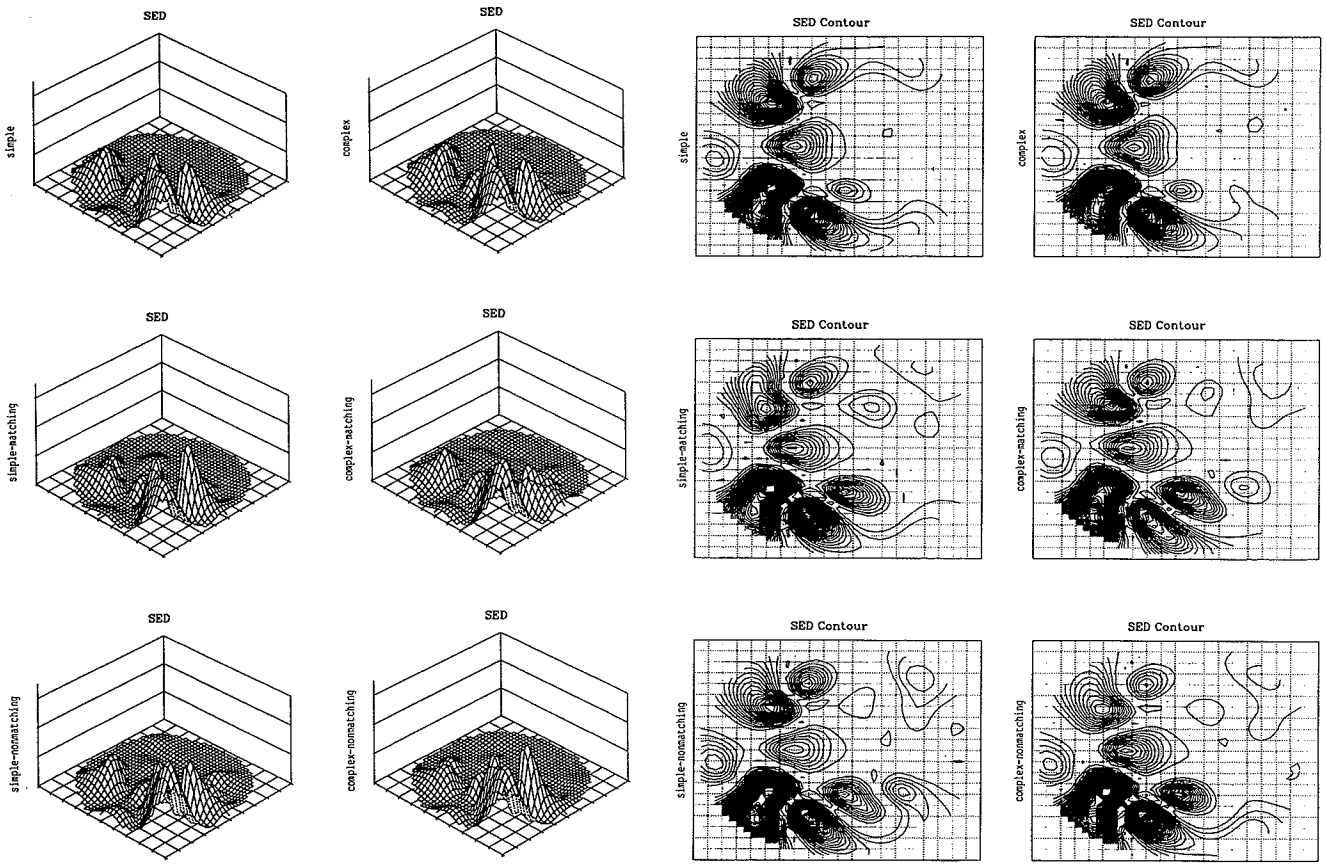

Figure 3 (left). SED fields on the *x*-*y* plane (looking from the back and right corner of the head), transformed from the latitude and longitude domain by $x = (\varphi * 2/\pi) * \cos(\theta)$ and $y = (\varphi * 2/\pi) * \sin(\theta)$ at SEC175 for the six cases. The order is the same as figure 2. Figure 3 (right) SED contours of the corresponding SED fields in figure 3 (left). The interval between two adjacent reference lines at the *x* (horizontal)-axis (the right side of the head) or *y* (vertical)-axis (the back side of the head) is 0.1.

appears in all six cases, but SEC375 appears only in the last four cases. The first two cases reflect stimulus perception and encoding, and the last four cases reflect stimulus comparison and recognition. (2) For SEC175, the SE to complex stimuli is larger than the SE to simple stimuli, and the SE to nonmatching stimuli is larger than the SE to corresponding matching stimuli. The complex patterns and the nonmatching patterns result in greater surface energy than the simple patterns and the matching patterns, respectively. (3) For SEC175, the SE for the first two cases is larger than for the last four cases; the latencies in the first two cases are about 5 to 15 ms longer than in the last four cases. (4) For SEC375 in the last four cases, the SE to any nonmatching case is larger than to corresponding matching cases; the latencies for any nonmatching cases are about 45 ms longer than for corresponding matching cases. This indicates that the nonmatching stimuli require more energy and time for comparison than the matching stimuli. (5) The patterns of the SE waves in the first two cases are the same. In the last four cases, the patterns of the SE waves for the two nonmatching stimuli are the same, and are also the same for the two matching stimuli. However, the patterns of the SE waves for the nonmatching and matching stimuli are different. (6) The largest pattern change, which corresponds to the largest information transmission and is indicated by the highest peak in the DSED wave, is at about 125 ms and takes about 50 ms duration for all 6 cases. A continuous SED field graph for this 50 ms interval indicates how the information is transmitted.

Figures 3 and 4 show the SED fields and their contours at SEC175 and SEC375 in the 6 cases. It is easy to see that: (1) the SE for SEC175 is mostly from the temporal regions in which the right posterior region demonstrates more energy than the left. This may be a characteristic of the brain activity involved in processing visual shape stimuli, and is consistent with single cell recordings in the inferior temporal cortex of monkeys which are known to encode information about shape and color of stimuli (Mikami and Kubota 1980; Riches et al. 1991; Miller et al.

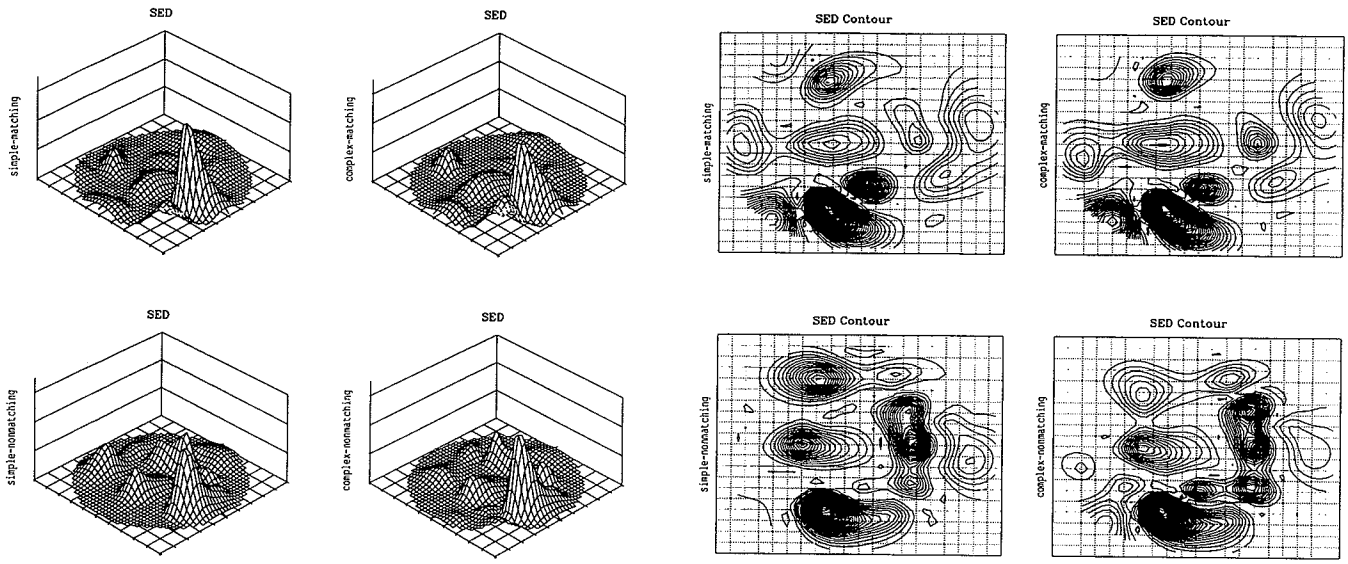

Figure 4. (left) SED fields on the the *x-y* plane at SEC375 for the last four cases: the simple-matching case is at the top left and the simple-nonmatching case is at the bottom left; on the right side are the corresponding two complex cases; Figure 4 (right) SED contours of the corresponding SED fields in figure 4 (left).

1991). (2) The SE for SEC375 is mostly from the temporal region in which again the right posterior region demonstrates more energy than the left. In addition, in nonmatching cases, the frontal fields are involved as well. This may indicate that the temporal region is involved in recognition processes of visual shape stimuli. The results regarding the involvement of the frontal field are new, and may represent the involvement of the frontal cortex in the mnemonic processing of different visual stimuli (Skelly et al. 1992).

Our findings indicate that the SE, SED and DSED represent an interesting and useful method which captures the cortical spatial and temporal properties of scalp recorded ERP's. Figures 5 to 7 show the waves of the absolute values of potentials recorded at electrodes CP5, P7, P3, O1, CP6, P8, P4, and O2 in the six cases. From them, we see that the patterns in the SE waves retain some important characteristics and properties present, as well as those obscured or absent, in the original recorded potentials at some electrode sites. Therefore, we may assume that the patterns in the SE waves retain important properties of the original recorded potential fields.

Conclusions

We proposed three new measures, the SE, SED and DSED. They and their local measures LSE, LSED and LDSED can be used in topographic component recognition and pattern recognition. They are different from the measures provided in the literature in their combined advantages: (1) reference independent, (2) free of any physical conductive model of the head, (3) represent a specific physical meaning of the scalp potential field, (4) include spatial information, (5) retain important spatial patterns and temporal elements of the original records, (6) allow comparisons in both the topographic and statistical domains among different subjects, time points, regions on the scalp as well as experimental conditions. These combined advantages are not present simultaneously in any single measure provided in the literature. Some of these advantages are rarely observed in the literature at all, namely: possessing a certain physical meaning of the scalp potential field, including spatial information, retaining important spatial patterns and temporal elements of the original records and allowing comparisons among different regions on the scalp. From the applications, we see that the patterns in both the SE waves and the SED fields are consistent in the same experimental conditions, and distinguishable in the different conditions. The surface energy components are physically meaningful, clearly identifiable, and retain the important properties present and smeared in the original recorded potential field. All of these support the contention that the SE, SED and DSED measures proposed here will be very useful tools in the analysis of both spatial and temporal properties of the recorded potentials in EEG and ERP's in the future.

Appendix

In order to derive the SCD field (2.4) from (2.1), we need the following results about the Laplacian operator

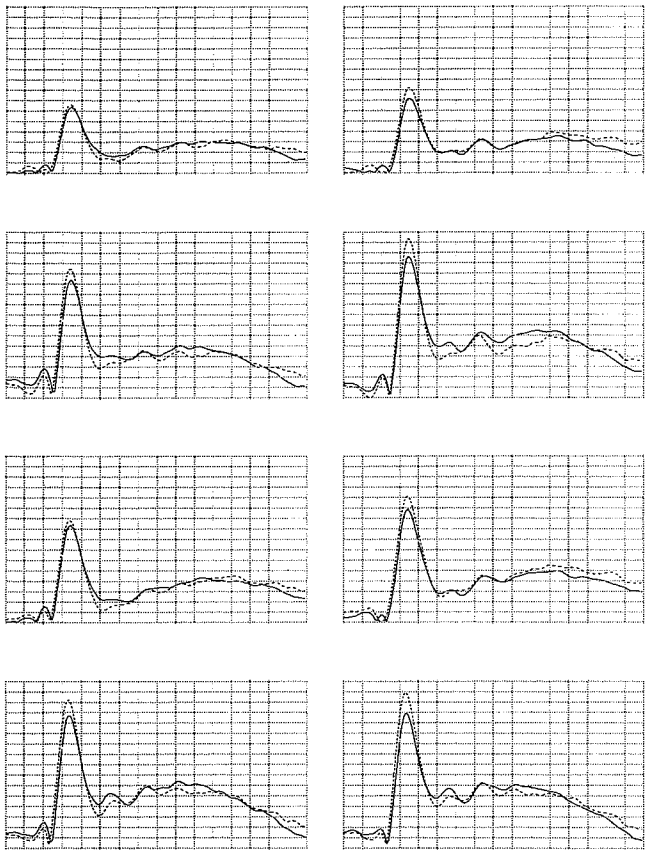

Figure 5. The waves of absolute values of potentials recorded at eight electrode sites in the simple and complex cases: CP5 at the top left, P7 at the second left, P3 at the third left and O1 at the bottom left; the corresponding electrodes at the right side are CP6, P8, P4 and O2, respectively. Solid lines are the simple cases; dashed lines are the complex cases. The interval between two adjacent reference lines at the time-axis (horizontal axis) is 50 ms.

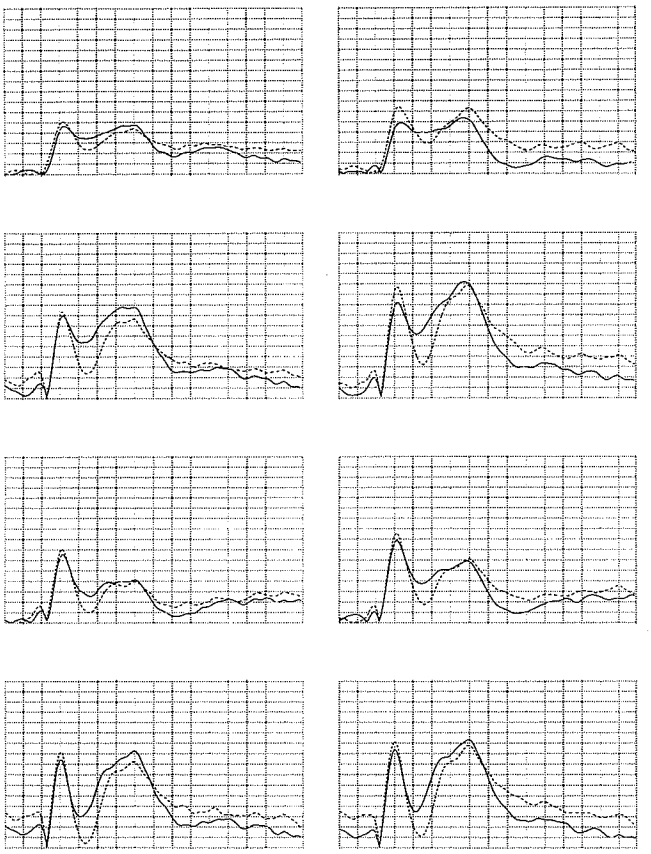

Figure 6. The waves of absolute values of potentials recorded at eight electrode sites in the simple-matching and complex-matching cases with the same order as figure 5. Solid lines are the simple-matching cases; dashed lines are the complex-matching cases. The interval between two adjacent reference lines at the time-axis is 50 ms.

under an orthogonal transformation of the coordinate system.

Let P(x, y, z) be a point on the surface of the scalp, (1, φ, θ)be the corresponding spherical coordinates of P and E (1, φ_0, θ_0) be the position of an electrode site on the scalp. We define a new rectangular coordinate system which is induced by E and determined by the following orthogonal matrix $\mathbf{U}$,

$$\boldsymbol{U} = \begin{pmatrix} cos(\varphi_0)\, cos(\theta_0) & -\sin(\theta_0) & sin(\varphi_0)\, cos(\theta_0) \\ cos(\varphi_0)\, sin(\theta_0) & cos(\theta_0) & sin(\varphi_0)\, sin(\theta_0) \\ -sin(\varphi_0) & 0 & cos(\varphi_0) \end{pmatrix} \tag{A.1}$$

In this new coordinate system, P has location (x_1, y_1, z_1), where

$$(x_1, y_1, z_1)^T = \boldsymbol{U}^T (x, y, z)^T \tag{A.2}$$

and E will lie on the z_1-axis at (0, 0, 1), where $\mathbf{U}^T$ is the transpose of $\mathbf{U}$. Let (1, φ_p, θ_p) be the corresponding spherical coordinates of P in this new coordinate system. Then it is clear that the latitude $\varphi_p = \gamma$ (P, E) of P is the angle between $\overrightarrow{OP}$ and $\overrightarrow{OE}$. It is well known that $P_n(cos\ (\varphi_p))$, $\cos(\theta_p)\ P^1_n\ (cos(\varphi_p))$ and $sin(\theta_p)\ P^1_n\ (cos\ (\varphi_p))$ are eigenfunctions of the Laplacian operator under this new coordinate system.

If we denote $\tilde{\Delta} \stackrel{def}{=} \frac{1}{\sin^2\varphi}\frac{\partial^2}{\partial\theta^2} + \frac{1}{\sin\varphi}\frac{\partial}{\partial\varphi}\ (sin\ \varphi \frac{\partial}{\partial\varphi})$ as the restriction of the Laplacian in 3-dimensional space to the surface of the sphere under the original coordinate

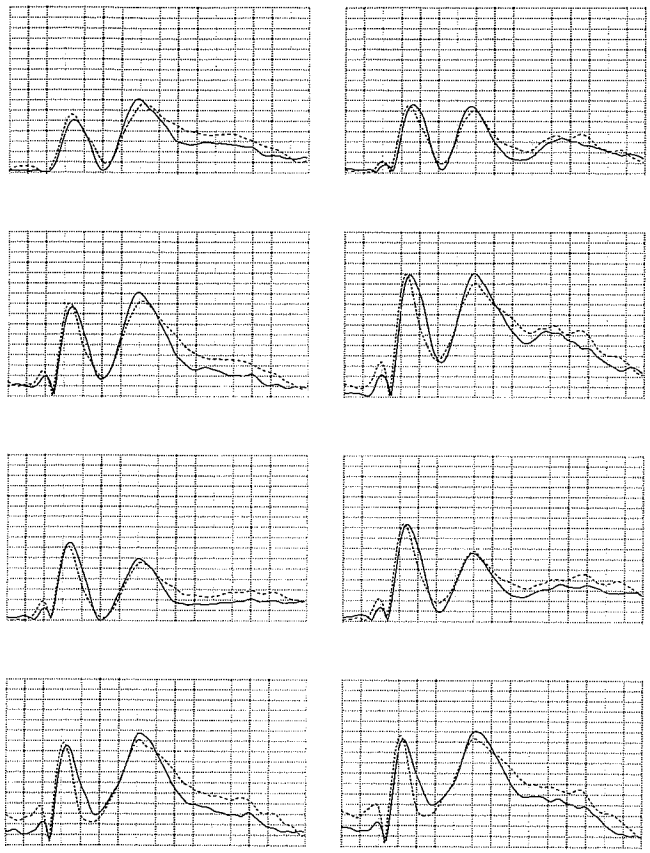

Figure 7. The waves of absolute values of potentials recorded at eight electrode sites in the simple-nonmatching and complex-nonmatching cases with the same order as figure 5. Solid lines are the simple-nonmatching cases; dashed lines are the complex-nonmatching cases. The interval between two adjacent reference lines at the time-axis is 50 ms.

system, then, by the definition and (2.1), the spherical scalp current density SSCD(P) at P will be given by

$$SSCD\,(P) = SSCD\,(x, y, z) = -\,\sigma_1 \tilde{\Delta} SSP\,(x, y, z)$$

$$= -\,\sigma_1 \sum_{i=1}^{q} c_i\, \tilde{\Delta}\, g\,(cos\,(\gamma\,(P, E_i))) \qquad \text{(A.3)}$$

where σ_1 is the conductivity of the scalp. Noting that in this expression, g contains the Legendre polynomials $P_n(\cos(\gamma(P, E_i)))$, but $\gamma(P, E_i)$ here is the latitude of P under the new coordinate system induced by E_i. Therefore, we have q latitudes defined by q different coordinate systems induced by q positions of electrodes. The aforementioned definition of the eigenfunctions is not directly applicable here. However, in the following lemma, we will prove that, under any orthogonal transformation such as inducing by E_i and defined in (A.1) and (A.2),

$$\tilde{\Delta} g\,(cos\,(\gamma\,(P, E_i))) = \tilde{\Delta}_{E_i}\, g(cos(\gamma\,(P, E_i))),\ \textit{for all } i \qquad \text{(A.4)}$$

where $\tilde{\Delta}_{E_i}$ is the restriction of the Laplacian in 3-dimensional space to the surface of the sphere under the coordinate system induced by E_i. Therefore, (A.3) can be written as, by the definition of the eigenfunctions and assuming $m > 2$,

$$SSCD(P) = \sigma_1 \sum_{i=1}^{q} c_i\, h\,(cos\,(\gamma\,(P, E_i\,))),$$

$$h\,(\cdot) = \frac{1}{4\pi} \sum_{n=1}^{\infty} \frac{2n+1}{n^{m-1}(n+1)^{m-1}}\ P_n\,(\cdot)$$

Therefore, we have (2.4) and (2.5).

Lemma

Let $\mathbf{U}$ be an orthogonal matrix, $(x_1, y_1, z_1)^{\mathrm{T}} = \mathbf{U}^{\mathrm{T}}(x, y, z)^{\mathrm{T}}$

$$\Delta \overset{def}{=} \frac{\partial^2}{\partial x^2} + \frac{\partial^2}{\partial y^2} + \frac{\partial^2}{\partial z^2}$$

be the Laplacian under the original coordinate system, and

$$\Delta_1 \overset{def}{=} \frac{\partial^2}{\partial x_1^2} + \frac{\partial^2}{\partial y_1^2} + \frac{\partial^2}{\partial z_1^2}$$

be the Laplacian under the new coordinate system determined by $\mathbf{U}$. Then

$$\Delta V\,(x, y, z) = \Delta_1 V\,(x_1, y_1, z_1)$$

for any twice differentiable function V.

Proof

Proof is direct by using the chain rule and the property of an orthogonal matrix.

References

Begleiter, H., Porjesz, B. and Wang, W. A neurophysiologic correlate of visual short-term memory in humans. Electroencephalography and Clinical Neurophysiology, 1993, 86:368-

376.
Devroye, L. A course in density estimation. Birkhauser, Boston, 1987.
Gevins, A.S. Correlation analysis. In: A.S. Gevins and A. Remond (Eds.), Methods of Analysis of Brain Electrical and Magnetic Signals. Elsevier, Amsterdam, New York, Oxford, 1987: 171-193.
Lehmann, D. Principles of spatial analysis. In: A.S. Gevins and A. Remond (Eds.), Methods of Analysis of Brain Electrical and Magnetic Signals. Elsevier, Amsterdam, New York, Oxford, 1987: 309-354.
Lehmann, D. and Skrandies, W. Reference-free identification of components of checkerboard evoked multichannel potential fields. Electroencephalography and Clinical Neurophysiology, 1980, 48: 609-621.
Mikami, A. and Kubota, K. Inferotemporal neuron activities and color discrimination with delay. Brain Res., 1980, 182: 65-78.
Miller, E.K., Li, L. and Desimone, R. A verbal mechanism for working and recognition memory in inferior temporal cortex. Neurosci Abstract, 1991, 2: 1377-1379.
Nunez, P. Electric fields of the brain - the neurophysics of EEG. Oxford University Press, New York, Oxford, 1981.
Nunez, P., Pilgreen, K.L., Westdorp, A.F., Law, S.K. and Nelson, A.V. A visual study of surface potentials and Laplacians due to distributed neocortical sources: computer simulations and evoked potentials. Brain Topography, 1991, 4: 151-168.
Perrin, F., Bertrand, O. and Pernire, J. Scalp current density: value and estimation from potential data. IEEE Trans. Biomed. Eng., 1987, 34: 283-288.
Perrin, F., Pernire, J., Bertrand, O. and Echallier, J.F. Spherical splines for scalp potential and current density mapping. Electroenceph. clin. Neurophysiol., 1989, 72: 184-187.
Riches, I.P., Wilson, F.A.W. and Brown, M.W. The effects of visul stimulation and memory on neurons of the hippocampal formation and the neighboring parahippocampal gyrus and inferior temporal cortex of the primate. J. Neurosci., 1991, 11: 1763-1779.
Skelly, J.P., Wilson, F.A.W. and Goldman-Rakic, P.S. Neurons in the prefrontal cortex of the macaque selective for faces. Soc. Neurosci. Abstr., 1992, 18: 1, 705.
Wahba, G. Spline interpolation and smoothing on the sphere. SIAM J. Sci. Stat. Comput., 1981, 2: 5-16.